Self-Trapped Interstitial-Type Defects in Iron

D. A. Terentyev,[1] T. P. C. Klaver,[2] P. Olsson,[3] M.-C. Marinica,[4] F. Willaime,[4] C. Domain,[3] and L. Malerba[1,*]

[1]*Nuclear Materials Science Institute, SCK-CEN, Boeretang 200, B-2400, Mol, Belgium*

[2]*School of Mathematics and Physics, Queen's University Belfast, Belfast BT7 1NN, Northern Ireland, United Kingdom*

[3]*Département MMC, EDF R&D, Les Renardières, 77250 Moret-sur-Loing, France*

[4]*Service de Recherches de Métallurgie Physique, CEA/Saclay, 91191 Gif-sur-Yvette Cedex, France*

(Received 14 September 2007; published 9 April 2008)

Small interstitial-type defects in iron with complex structures and very low mobilities are revealed by molecular dynamics simulations. The stability of these defect clusters formed by nonparallel ⟨110⟩ dumbbells is confirmed by density functional theory calculations, and it is shown to increase with increasing temperature due to large vibrational formation entropies. This new family of defects provides an explanation for the low mobility of clusters needed to account for experimental observations of microstructure evolution under irradiation at variance with the fast migration obtained from previous atomistic simulations for *conventional* self-interstitial clusters.

DOI: 10.1103/PhysRevLett.100.145503 PACS numbers: 61.72.J−, 61.72.Bb, 61.80.Az, 61.82.Bg

The safety of existing and future nuclear power plants largely depends on the radiation resistance of the chosen structural materials, determined by their microstructure evolution under irradiation. With a view to developing reliable numerical multiscale models of the microstructural changes produced by irradiation, one of the key issues, especially in body-centered cubic (bcc) metals, is that of the migration properties of self-interstitial atoms (SIA) and their clusters [1–7]. The case of iron, the base material for steels, is especially important because steels are widely used in nuclear reactors, and the properties of interstitial defects in this metal are peculiar and their physics is not yet completely understood. Experimentally observed SIA loops in iron may have both $\frac{1}{2}\langle 111\rangle$ and $\langle 100\rangle$ Burgers vectors [6,8]. For the single SIA, experiments [9] and density functional theory (DFT) calculations [2,4] agree on a $\langle 110\rangle$ dumbbell configuration, at variance with the $\langle 111\rangle$ crowdion found in other bcc metals [3]. Initially it was believed that small SIA clusters in iron had to be collections of parallel $\langle 110\rangle$ dumbbells. The formation of the observed $\frac{1}{2}\langle 111\rangle$ and $\langle 100\rangle$ loops was explained as the unfaulting of $\langle 110\rangle$ clusters above a critical size [10]. However, the use of many-body potentials (MBPs) in molecular dynamics (MD) studies suggested these clusters to be collections of parallel $\langle 111\rangle$ crowdions instead, capable of gliding one-dimensionally (1D) with very small migration energy (tens of meV) [5,7,11]. This is qualitatively consistent with recent *in situ* transmission electron microscopy (TEM) experiments, showing that not only $\frac{1}{2}\times\langle 111\rangle$ SIA loops, but also $\langle 100\rangle$ loops, can move in ultra pure Fe above 450 K [6]. However, while accepted microstructure-evolution models succeeded in describing void swelling assuming high 1D mobility of at least part of the SIA clusters [12], other models showed that, in iron, agreement with experimental observations can only be obtained if the MD calculated high mobility of SIA clusters is artificially reduced, by either introducing traps [13] or even postulating their immobility [2].

Recently, DFT calculations showed that clusters of up to four SIAs are more stable as collections of parallel $\langle 110\rangle$ dumbbells than $\langle 111\rangle$ crowdions, with accordingly larger migration energy [14]. This is due to a higher energy difference between the $\langle 111\rangle$ crowdion and the $\langle 110\rangle$ dumbbell than was found with early MBPs [4] (~ 0.7 eV versus less than 0.3 eV). Using this information, more reliable MBPs for iron have been developed [15,16]. However, the revisited stability and higher migration energy of small $\langle 110\rangle$ clusters does not remove the need for traps for the fast migrating clusters in microstructural evolution models [13].

MD simulations of cascades in iron using an early MBP showed that SIA-cluster configurations made of nonparallel dumbbells form spontaneously [17]. MD studies with a more recent MBP [16] confirmed the formation of SIA clusters in nonparallel configurations (NPCs), not only in cascades [18], but also during cluster migration at high temperature [7], thereby suggesting that they are thermally stable. The specificity of these *self-trapped* configurations is that no simple mechanism exists whereby they can migrate, as they need first to unfault to parallel configurations.

In this Letter, the stability of some NPCs is studied by combining MD and lattice dynamics, using the MBP applied in Refs. [7,18] and DFT methods. DFT provides the ground states at 0 K, while with the MBP the study is extended to finite temperatures, looking tentatively at unfaulting mechanisms, too. We show that the thermal stability of these NPCs may provide an explanation for many of the still unclear issues briefly outlined above.

DFT calculations were performed with the SIESTA code in the Perdew-Burke-Enzerhof generalized gradient approximation (GGA), with a real-space grid spacing equal to 0.067 Å using a norm-conserving pseudopotential. Details on the localized basis set and its validation can be found in Ref. [14]. For comparison, calculations were also carried out with VASP [19], a plane-wave code employ-

ing the projector augmented wave (PAW) method [20]. Standard VASP potentials were used, with the Perdew-Wang parametrization in the GGA. The plane-wave energy cutoff was set to 300 eV. With both codes, the calculations were performed with 8 valence electrons per Fe atom and with spin polarization, the Brillouin zone being sampled by meshes of $3 \times 3 \times 3$ k points, in the Monkhorst-Pack scheme. The atomic positions of the defects were relaxed in 250 atom supercells, held at constant equilibrium volume during relaxation in VASP, while volume expansion at constant pressure was allowed in SIESTA. Inserting multiple SIAs in a fixed volume introduces substantial stresses; however, for di-interstitials it was shown [4] that the energy shifts between calculations in supercells with different small sizes or different relaxation conditions (e.g., constant volume vs constant pressure) are highly systematic. The relative stability of different configurations is therefore not expected to depend on the applied conditions and box size also for larger numbers of defects. We estimated that for numbers of SIAs larger than 2 the nonsystematic shift of the energies may introduce energy difference errors <0.1 eV.

MBP calculations were used to assess the stability of the NPCs at finite temperature, by calculating the associated vibrational formation entropy in the harmonic approximation (lattice dynamics) [21] and by monitoring in MD simulations the time the clusters spend in NPCs versus temperature, so as to also observe the unfaulting mechanisms. Full convergence of static formation energies with the MBP was ensured by using a 2000 atom box. The same cell size was also used in MD calculations, while 1024 atoms cells were used for the vibrational entropy calculations.

In Fig. 1 the cluster configurations containing from two to four SIAs investigated in this study are pictorially shown. The static formation energies, obtained by the different methods, as well as the MBP formation entropies, are indicated. The configurations generally accepted as most stable in this range of sizes consist of first nearest neighbor, parallel ⟨110⟩ dumbbells [7,14]. The formation energies of these configurations, denoted as $I2_{\langle 110\rangle}$, $I3_{\langle 110\rangle}$, and $I4_{\langle 110\rangle}$, are thus used here as references. During migration, the dumbbells of these ⟨110⟩ clusters perform translation-rotation jumps, so the clusters experience transformations between equivalent ⟨110⟩ states, via configurations in which the dumbbells are temporarily not parallel [7]. Other known possible SIA-cluster configurations consist of parallel ⟨111⟩ crowdions (denoted as $I2_{\langle 111\rangle}$, $I3_{\langle 111\rangle}$, and $I4_{\langle 111\rangle}$). These configurations, if stable, migrate by fast 1D glide [5,7,11]. Of all *a priori* possible NPCs, those in Fig. 1 (denoted as $I2_{\mathrm{np}}$, $I3_{\mathrm{np}}$, and $I4_{\mathrm{np}}$) spontaneously appeared in MD studies carried out with the MBP used in this Letter [7,18] ($I2_{\mathrm{np}}$ was also reported in a previous study with a different MBP [17]). All of them have been found in this work to be stable at zero Kelvin, i.e., to correspond to local energy minima, independently of the

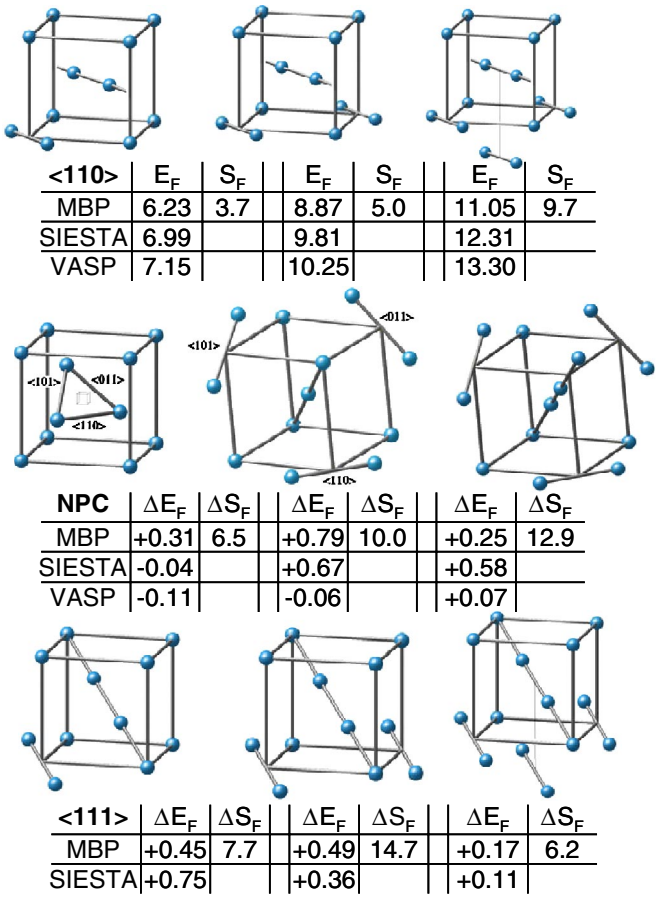

FIG. 1 (color online). SIA-cluster configurations and corresponding statically calculated properties (E_f, ΔE_f: formation energy and formation energy difference compared to ⟨110⟩ configuration; S_f, ΔS_f: formation entropy and formation entropy difference compared to ⟨110⟩ configuration; energies are in eV, entropies in k_B = Boltzmann's constant). For comparison, ⟨111⟩ configurations and their ΔE_f (using results from Ref. [12]) are also given.

calculation method. $I2_{\mathrm{np}}$ can be described as three atoms sharing a lattice site, forming a triangle with ⟨110⟩ oriented sides on a {111} plane. $I3_{\mathrm{np}}$ is a ring that lies on a {111} plane, formed by three nonparallel ⟨110⟩ dumbbells, whose centers are slightly offset from the corresponding lattice sites, toward the center of the ring. $I4_{\mathrm{np}}$ is the same ring as in $I3_{\mathrm{np}}$, with the addition of a ⟨111⟩ crowdion perpendicular to the {111} plane of the ring, located one nearest neighbor distance away from it.

Figure 1 reveals that quantitative differences exist depending on the calculation method. Broadly, SIESTA results are well reproduced by the MBP (with the exception of $I2_{\mathrm{np}}$). Firstly, we shall focus on MBP-SIESTA results and then describe the qualitative differences observed with VASP.

According to SIESTA, $I2_{\mathrm{np}}$ is essentially degenerate with $I2_{\langle 110\rangle}$, both being much more stable than $I2_{\langle 111\rangle}$. Unfortunately the MBP cannot grasp the first feature, and this is the defect for which the MBP results are therefore

the least reliable. On the other hand, according to both SIESTA and the MBP, $I3_{np}$ and $I4_{np}$ are high energy states at zero Kelvin, even higher than $I3_{\langle 111\rangle}$ and $I4_{\langle 111\rangle}$. In a previous MBP study of the mobility of SIA clusters [7] these configurations were, however, clearly detected at high temperature (> 600 K). Their appearance in spite of the high excess formation energy, particularly in the case of $I3_{np}$, can be explained by their formation entropy, which is significantly larger than for the reference state and comparable to that of $\langle 111\rangle$ configurations (Fig. 1). These high excess entropies are due to low frequency resonant modes. For the $\langle 111\rangle$ clusters these modes are either libration modes or translation modes corresponding to the 1D easy glide in the $\langle 111\rangle$ direction; their frequencies are much lower than in $\langle 110\rangle$ clusters. The resonant modes of the NPC clusters have complex polarizations; their common feature is that they combine a translation within the $\{111\}$ plane of the interstitial-type defect and $\langle 111\rangle$ displacements in opposite directions of nearest neighbor atoms separated by the defect.

Simple estimates based on our MBP data reveal that the free energy of formation of $I2_{np}$, $I3_{np}$, and $I4_{np}$ becomes lower than that of $\langle 110\rangle$ configurations above, respectively, 550, 920, and 225 K. Thus, the three of them are expected to be the most favorable configurations at sufficiently high temperature. For comparison, the corresponding $\langle 111\rangle$ configurations become favored over the $\langle 110\rangle$ configurations at, respectively, 680, 390, and 320 K.

We also used the MBP to assess the lifetime of the NPCs of Fig. 1 versus temperature, once formed, by monitoring these configurations and stopping the chronometer when they unfaulted into a parallel configuration and subsequent migration occurred. To allow for the stochastic nature of the onset of the transformation, the same simulation was repeated 20 times for each temperature. The results are shown in Fig. 2. The lifetime of $I2_{np}$ and $I3_{np}$ is fairly short, remaining below 1 ns above, respectively, 450 and 300 K. In the case of $I4_{np}$, however, data points could be only collected in a high temperature range, as at lower temperature this NPC was never seen to unfault, even after 20 ns. Moreover, the slope of the $I4_{np}$ data points versus $1/k_BT$, which equals the effective activation energy for unfaulting assuming Arrhenius behavior, is extremely high. Within the large data scatter, we could estimate unfaulting energies of 0.43 ± 0.08, 0.15 ± 0.04, and 1.68 ± 0.29 eV for, respectively, $I2_{np}$, $I3_{np}$, and $I4_{np}$. The type of unfaulting depends on cluster size. In $I2_{np}$ unfaulting proceeds via the formation of a configuration in which two $\langle 110\rangle$ dumbbells are perpendicular to each other and unfaulting to $I2_{\langle 111\rangle}$ never occurs. $I3_{np}$ also unfaults only to $I3_{\langle 110\rangle}$, via on site rotation of two dumbbells, whereas $I4_{np}$ unfaults to the $I4_{\langle 111\rangle}$ glissile configuration. The reason for the surprisingly large unfaulting energy of $I4_{np}$ can be traced down to a two-step transition process, at least with this MBP. First, the central crowdion glides further away from the $I3_{np}$ ring,

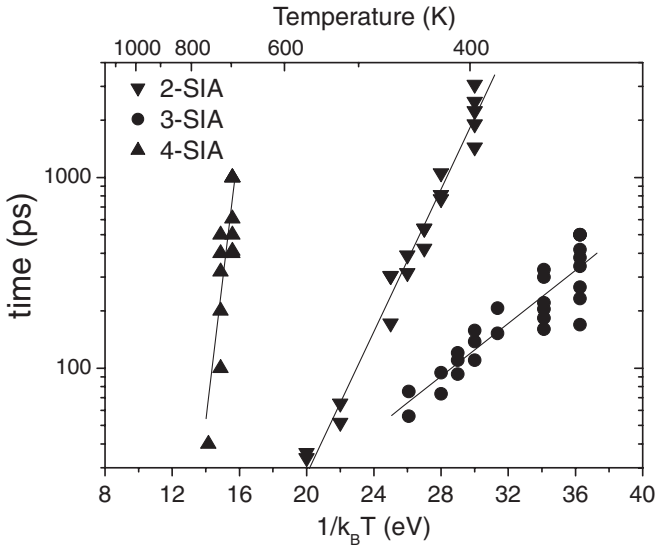

FIG. 2. Lifetime of the NPCs in dynamic simulations with the MBP, in Arrhenius-like representation.

then the latter unfaults to $I3_{\langle 111\rangle}$, and finally the crowdion rejoins it. Such a mechanism was systematically observed at different temperatures. Thus, the unfaulting requires the partial emission of the central crowdion. Accordingly, the unfaulting energy is on the order of the binding energy of the crowdion to the 3-SIA cluster. Although these numbers must be considered as only indicative, they suggest that 4-SIA clusters may spend up to a few ms in a NPC at 600 K (a typical operating temperature for a nuclear reactor). Even if for the rest of their life they migrated by fast, 1D glide along $\langle 111\rangle$ directions [5,7,11], their effective migration energy would be significantly affected, and they would remain immobile for time spans sufficiently long to have an impact on the microstructure evolution.

The NPCs in Fig. 1 possess two important properties: they are highly symmetric and they can be used as elementary blocks to build clusters of larger size, whose migrating properties, as is the case for $I4_{np}$, are expected to be different from those of the corresponding parallel configurations. In particular, $I5_{np}$, $I6_{np}$, and $I7_{np}$ clusters can be built by substituting each of the three $\langle 110\rangle$ dumbbells in the ring of $I4_{np}$ with $I2_{np}$ configurations. Larger clusters can be formed by further merging $I2_{np}$ configurations. Such clusters, particularly $I5_{np}$, $I7_{np}$, $I8_{np}$, and $I11_{np}$, have been identified in MD cascade studies at 300 K with the MBP [18], and $I5_{np}$ was also found to form spontaneously during free migration of 5-SIA clusters [7]. In addition, a platelet containing $\langle 100\rangle$ dumbbells can be built by proper juxtaposition on different $\{111\}$ planes of 2_{np} configurations, as shown in Ref. [22]. Our studies with the MBP suggest that the formation of NPCs built by $I2_{np}$ blocks is promoted at high temperature, due to high formation entropy. Their formation in iron is expected to be even more favorable than as observed in MBP studies, considering that DFT predicts the $I2_{np}$ to be the ground

state. The VASP results, moreover, suggest the NPCs to be the ground state ($I2_{np}$), or degenerate with it ($I3_{np}$ and $I4_{np}$), for *all* SIA clusters considered in this study (see Fig. 1). Calculations performed with VASP using ultrasoft pseudopotentials instead of PAW suggest that this discrepancy between DFT methods may be attributed to limitations in the pseudopotential approximation. An exhaustive study on this point is, however, beyond the scope of this Letter. The PAW calculations are more accurate, especially in magnetic systems [20]; thus, our statement about the existence and stability of SIA clusters in NPCs becomes even more valid in the light of PAW results.

According to current knowledge from atomistic simulations in Fe, clusters of five SIAs and larger have ⟨111⟩ ground state configurations and move via 1D glide [5,7,11,14], in qualitative agreement with TEM studies [6]. But if, as suggested by the present and previous work [7,17,18], clusters larger than 4 SIA can also exist in NPCs, then the formation and growth up to sizes visible by TEM of clusters in self-trapped configurations, possible nuclei of ⟨100⟩ platelets, cannot be ruled out. Fully reliable studies of large clusters in NPCs and their migration properties exceed the limit of currently available modelling tools. They are not accessible to DFT and no existing MBP is capable, to our knowledge, of predicting the $I2_{np}$ as ground state for the 2 SIA, which is here postulated to be the fundamental building block for large NPCs. However, the evidence here provided from the combination of different techniques allows us to postulate the existence, in iron and in diluted bcc iron-based alloys, of two classes of intermediate-size SIA clusters, characterized by very different migration properties: (1) 1D glissile clusters (⟨111⟩ configurations) and (2) self-trapped clusters built from $I2_{np}$ and/or $I3_{np}$ blocks. Depending on temperature, the latter eventually become mobile via unfaulting to ⟨111⟩ configurations, but may also consolidate into a ⟨100⟩ configuration. Such a mechanism may explain why, in microstructural evolution models, no agreement with experiments is reached if all SIA clusters are allowed to be highly mobile.

In summary, the combination of computer simulation techniques has revealed the existence of unexpected configurations of self-interstitial clusters in iron, formed by nonparallel dumbbells. The properties of these configurations provide a new picture, which clarifies a long-standing debate on the properties of SIA clusters in iron. Because of their intrinsic low mobility they are candidates to be the immobile clusters, the existence of which has to be assumed to account for experiments. Second, they may act as nuclei for ⟨100⟩ interstitial loops observed specifically in iron. Finally, their unusually large formation entropy yields a strong temperature dependence of their stability with respect to other configurations, suggesting a temperature dependence of SIA-cluster properties to be taken into account in the interpretation of available experiments using multiscale approaches, as well as in the design of new experiments and development of new models.

This work was performed in the framework of the PERFECT IP, supported by the European Commission under Contract No. FI6O-CT-2003-5088-40.

*lmalerba@sckcen.be

[1] I. Cook, Nat. Mater. **5**, 77 (2006).
[2] C. C. Fu, J. Dalla Torre, F. Willaime, J. L. Bocquet, and A. Barbu, Nat. Mater. **4**, 68 (2005).
[3] D. Nguyen-Manh, A. P. Horsfield, and S. L. Dudarev, Phys. Rev. B **73**, 020101(R) (2006).
[4] C. Domain and C. S. Becquart, Phys. Rev. B **65**, 024103 (2001); C.-C. Fu, F. Willaime, and P. Ordejón, Phys. Rev. Lett. **92**, 175503 (2004).
[5] J. Marian, B. D. Wirth, A. Caro, B. Sadigh, G. R. Odette, J. M. Perlado, and T. Diazde la Rubia, Phys. Rev. B **65**, 144102 (2002); Yu. N. Osetsky, D. J. Bacon, A. Serra, B. N. Singh, and S. I. Golubov, Philos. Mag. **83**, 61 (2003).
[6] K. Arakawa, M. Hatanaka, E. Kuramoto, K. Ono, and H. Mori, Phys. Rev. Lett. **96**, 125506 (2006).
[7] D. A. Terentyev, L. Malerba, and M. Hou, Phys. Rev. B **75**, 104108 (2007).
[8] B. L. Eyre and A. F. Bartlett, Philos. Mag. **12**, 261 (1965).
[9] P. Ehrhart, K. H. Robrock, and H. R. Schober, in *Physics of Radiation Effects in Crystals*, edited by R. A. Johnson and A. N. Orlov (Elsevier, Amsterdam, 1986) p. 63, and references therein.
[10] B. L. Eyre and R. Bullough, Philos. Mag. **12**, 31 (1965).
[11] A. F. Calder and D. J. Bacon, J. Nucl. Mater. **207**, 25 (1993); N. Soneda and T. Díaz de la Rubia, Philos. Mag. A **78**, 995 (1998); **81**, 331 (2001).
[12] S. I. Golubov, B. N. Singh, and H. Trinkaus, J. Nucl. Mater. **276**, 78 (2000), and references therein.
[13] C. Domain, C. S. Becquartand, and L. Malerba,J. Nucl. Mater. **335**, 121 (2004).
[14] F. Willaime, C. C. Fu, M. C. Marinica, and J. Dalla Torre, Nucl. Instrum. Methods Phys. Res., Sect. B **228**, 92 (2005).
[15] M. I. Mendelev, S. Han, D. J. Srolovitz, G. J. Ackland, D. Y. Sun, and M. Asta, Philos. Mag. **83**, 3977 (2003).
[16] G. J. Ackland, M. I. Mendelev, D. J. Srolovitz, S. Han, and A. V. Barashev, J. Phys. Condens. Matter **16**, S2629 (2004).
[17] F. Gao, D. J. Bacon, Yu. N. Osetsky, P. E. J. Flewitt, and T. A. Lewis, J. Nucl. Mater. **276**, 213 (2000).
[18] D. Terentyev, C. Lagerstedt, P. Olsson, K. Nordlund, J. Wallenius, C. S. Becquart, and L. Malerba, J. Nucl. Mater. **351**, 65 (2006); D. Terentyev, Ph.D. dissertation, Université Librede Bruxelles, Belgium, 2006.
[19] G. Kresse and J. Hafner, Phys. Rev. B **47**, 558 (1993); G. Kresse and J. Furthmuller, Phys. Rev. B **54**, 11 169 (1996).
[20] G. Kresse and D. Joubert, Phys. Rev. B **59**, 1758 (1999).
[21] M.-C. Marinica and F. Willaime, Diffus. Defect Data, Pt. B **129**, 67 (2007).
[22] D. Terentyev, L. Malerba, P. Klaver, and P. Olsson (to be published).